Submitted to Tectonics - February 14, 1989

MULTIPLE STRIKE SLIP FAULTS SETS:

A CASE STUDY FROM THE DEAD SEA TRANSFORM

Hagai Ron

The Institute for Petroleum Research and Geophysics

Holon, Israel

Amos Nur

Department of Geophysics, Stanford University, California, USA

Y. Eyal

Department of Geology, Beer Sheva University, Israel

ABSTRACT

In many strike slip tectonic settings, large rotations of crust blocks about vertical axes have been inferred from paleomagnetic data. These blocks are bounded by sets of parallel faults which presumably accommodate the relative motion between the blocks as regional deformation progress. A mechanical model by Nur et al., (1986) suggests that rotations greater than $\varnothing_c = 25°$ to 45° must be accommodated by more than one set of faults, with angle $\varnothing_c$ between their direction, consequently the sum of the angles between sets must be roughly equal to the total tectonic material rotation. To test this model we investigated the fault geometry and field relation of fault sets in the Mt. Hermon area in northern Israel, where paleomagnetic declination implies data $69° \pm 13°$ counterclockwise block rotation. The statistical and field relation analysis of over 315 faults shows that the faulting is predominantly right lateral strike slip consisting of three distinct sets. The oldest set strikes 253°, the second oldest set strikes 293° and the youngest strikes 339°. This last direction is consistent also with the current north-south direction of the maximum principle stress axis. The angle $\varnothing_c$ between the first and second sets is 39° and between the second and third sets 46°, in good agreement with the $\varnothing_c$ angle predicted from mechanical considerations. The sum of the two angles is 85° CCW, in good agreement with the $69° \pm 13°$ CCW paleomagnetically derived rotation. The results suggest specifically that the sequential development of multiple intersecting fault sets is responsible for the faulting in the Mt. Herman area; and generally that the model of block rotation with multiple faults provides very good simple rules for analyzing very complex fault patterns.

INTRODUCTION

In a seminal paper, Freund (1974) explored the kinematics of rotations of crustal blocks bounded by faults in sets. In his analysis, Freund has shown that the *sense* of

these rotations is controlled by the orientation of the faults within a given set relative to the principal direction of tectonic shortening, whereas the *magnitude* of the rotation of crustal blocks and their bounding faults is related to the magnitude of crustal shortening or extension.

There is growing evidence that block rotation due to crustal shortening and extension is widespread: For example, Ron et al. (1984) showed that adjacent domains of clockwise and counterclockwise rotations occur in the same tectonic setting of northern Israel, depending on the orientation of the active faults. Similar models were given for the Mojave area in California (Garfunkel, 1974), central America, (Manton, 1987), Alaska (Stamatokos et al., 1988), the Lake Mead, Nevada, region (Ron et al., 1986).

Freunds model implies that as blocks rotate, their bounding faults rotate away from their optimal direction of slip. When this rotation becomes sufficiently large, these faults lock up (Nur et al., 1986). Further crustal deformation must then be accommodated by a set of new faults, more favorably oriented to the principal direction of regional deformation. As a result, domains of multiple sets must form in which the younger faults systematically offset the older ones. The existence of such multiple sets thus provides a rigorous test for Freund's block rotation model. Although a few cases of multiple sets have been studied (Nur et al., 1986, Ron et al, 1986, Nur et al., in press), the evidence is still sparse. The purpose of this paper is to report on a new case of multiple fault sets and the evidence that they were formed sequentially through the process of large rotations of blocks in domains.

KINEMATICS AND STRESS ON ROTATING FAULTS

A key aspect of Freund's model is that blocks rotate counterclockwise (CCW) when slip is right handed, and clockwise (CW) when slip is left handed. When several

domains of fault sets exist - left and right handed, the model predicts relative rotations between the CCW and CW domains. It was shown by Nur et al., (1986) that when a faults of sets rotates away from the original and optimal direction of failure $\varnothing_o$ relative to the maximum stress, the shear stress acting on the fault plane decreases and the normal stress increases until it becomes locked. Thus, beyond a critical angle of rotation $\varnothing_c$ a new fault set is required more favorably oriented relative to the stationary direction of maximum stress. The faults in this new set will offset (Figure 1) the now locked faults of the older set.

The value of the predicted angle $\varnothing_c$ between the old and new fault directions was shown by Nur et al., (1986) to fall in the range of 25° up to 45°, for the extreme cases of coefficient of friction $\mu = 0$ or fracture strength to rock strength ratio $S_1/S_0 = 0$. The value $\varnothing_c = 45°$ is the upper premissible limit of block rotation (from the optimal failure direction which can be accommodated by a single set of faults).

The values $\varnothing_c = 25°$ to 45° are significantly lower than many reported rotations inferred for rocks insitu from paleomagnetic declination anomalies. If the analysis of Nur et al., (1986) is correct, than paleomagnetically derived rotations larger than 45° must involve more than one set of rotating faults. The existence of multiple sets in situ would, therefore, provide a direct test of the entire block rotation concept.

To test the model, we have carried out a detailed structural study of a carefully selected area in the Mt. Hermon region of northern Israel. Previously obtained paleomagnetic declination data in this region (Ron 1987) indicate a $69° \pm 13°$ counter-clockwise rotation. The hypothesis to be tested in this paper is wether the deformation associated with this rotation was accommodated by more than one set of faults. These faults must show right lateral strike slip and angles $\varnothing_c$ between them must fall in the range 25° to 45° or so.

REVIEW OF PALEOMAGNETIC RESULTS

Paleomagnetic results from the Mt. Hermon regions at the restraining bend of the Dead Sea transform plate margins were obtained by Gregor (1974) and Ron (1987) repetidly. The results have clearly demonstrated that crustal deformation was accommodated by horizontal fault and block rotation (Figure 2a). The data was obtained from both sides of the plate boundary: Paleomagnetic results from Early Cretaceous volcanic rocks obtained from Lebanon to the west, reveal anomalous paleomagnetic declinations which imply $55.6° \pm 10.4°$ *counterclockwise* rotation about a vertical axis (Gregor et al., 1974) - Ron's (1987) study in the Mt. Hermon area to the east yield a similar anomalous paleomagnetic declination with a $69° \pm 13°$ *counterclockwise* rotation about a vertical axis.

Two relevant links to the multiple fault set model are obvious: If block rotate a la Freund then the counterclockwise *sense* of rotation must be associated with right lateral strike slip (Freund, 1974, Ron et al., 1984), and the larger than 25° to 45° *magnitude* of rotation requires that more than one set of right lateral faults is involved in the rotation (Nur et. al., 1986).

STRUCTURAL STUDY

Mt. Hermon is situated at an oblique segment of the Dead Sea transform (Figure 2a) in a configuration similar to the transverse ranges in Southern California. This geometry gives rise to a transpressive regime normal to the plate boundary (Freund et al., 1970; Hancock and Atiya, 1979, Garfunkel, 1981) involving both folds and faults. The magnitude of shortening achieved by folding is only about 10% of the total shortening anticipated as a consequence of the left lateral displacement along the north-south Dead Sea transform colliding against the northeast trending Yammuneh segment (Figure 2a). Most of the deformation has presumably been accommodated by the

intricate network of west to north-west trending right lateral strike slip faults (Figures 2b, c; Ron, 1987). Because of good fault exposure and the existance of paleomagnetic data, this area was selected by us a for a detailed study to determine in situ fault plane orientations, fault rakes (slip vectors), and the sense of displacements, to determine whether faulting here is by multiple sets of faults which cross cut each other as expected from the block rotation model.

Data obtained from 315 faults include fault plane dip and strike, trend and plunge of the fault rake (fault slip vector) and sense of displacement whenever possible using field criteria such as discussed by Eyal and Reches (1983) and Angelier et al., (1985).

GEOMETRICAL ANALYSIS OF FAULT PATTERNS

We consider four aspects of the fault population data (a) the lower hemisphere projection of normals to the fault planes; (b) rose diagrams of pole trends; (c) rose diagrams of a fault dips; and (d) rose diagram of fault rakes (Figure 3, a to d).

The results show that over 80% of the mapped faults are vertical or subvertical with horizontal or subhorizontal rakes, and are therefore strike slip faults. The orientation distribution (Figure 3a, b) however, does not reveal clear clustering of fault types. Consequently we have next deleted all those faults for which the sense of slip is unknown. The remaining faults were then separated statistically into right slip and left slip groups. Fault normal stribution for the right lateral (Figure 4a) and for the left lateral (Figure 6a) faults were next plotted to show the number and orientation distribution of these faults. The trend distributions of both the right lateral (Figure 4b) and left lateral (Figure 6b) faults reveal that each group consists of three distinct sub groups or sets: The orientation and the statistical parameters of each right lateral fault sub group, calculated using Fisher's (1953) statistics are summarized in Figures 5 and 7 and in Table 1.

The results reveal that the right lateral faults make up over 70% of all the mapped faults, suggesting that most of the deformation in this area was accommodated by right lateral slip. This is in good agreement with the earlier model by Ron (1987) which requires that the dominant crustal deformation here is by right lateral slip on distributed fault sets. The results are of course consistent also with paleomagnetic data which imply from declination anomelies counterclockwise rotation (Figure 2b, c).

CROSS CUTTING RELATIONS

How are the three sets of right lateral strike slip faults related? The presence of three distinct sets of right lateral strike slip faults (Figure 10a) does not by itself verify that they are multiple sets. To fit our defenition of multiple sets the following relations exist insitu:

a) cross-cutting between the sets must be sequential as illustrated in Figure 1.

b) The angle between the youngest and oldest sets must have the same sense and the same magnitude as the paleomagnetically inferred total rotation.

To nail down the time relationship between the sets we chose an exceptionally well exposed outcrop near Neve Ativ, (NA) of about 500 m^2 in which excellent fault data were collected. Analysis of the faults in this outcrop was performed (Figures 8 and 9 and Table 1) yielding very similar results (Figure 10b). to the entire Mt. Hermon area (Figure 10a), This suggests that the outcrop is fairly representative of the entire region, the cross-cutting relations of the three right lateral sets of faults NA1, NA2, and NA3 in this outcrop were carefully determined:

a) The faults in the 256° trending set (NA-1) are always offset by the faults of the 333° trending set (NA-3).

b) The faults in 283° trending set (NA-2) offset the faults of the 256° trending set (NA-1) and form boudins of calcite fill of these faults.

These cross cutting relations imply that the oldest of the sets strikes 256°, the second oldest strikes 283° and the youngest strikes 333°. Furthermoore the orientation of the youngest set is coincident with the optimal present direction of faulting associated with the current north-south maximum horizontal compression (Ben Menahem et al, 1976; Joffe and Garfunkel, 1987).

As shown earlier, Nur's et al., (1986) block rotation model predicts that the angle between two consecutive sets of faults should fall in the range of 25° to 45°. Our field results yield a mean angle $\varnothing_{12}=39°$ between the first and second sets, and the $\varnothing_{23}=46°$ between the second and third sets (see Table 1) in good agreement with the values predicted by the mechanical model of rotating faults.It is noteworthy that the angle between the second and third sets is about the maximum value permitted. This high value may be due to low effective normal stress, perhaps associated with high pore pressure during this deformational phase.

Finally, the sum of the two angles $\varnothing_{12}$ and $\varnothing_{23}$ is 85°, a value which is in reasonable agreement with the paleomagnetically derived total rotation of $69°\pm13°$ (Ron, 1987).

SUMMARY

In the study reported here we combined paleomagnetic and structural data to test in the Mt. Hermon area the validity of our model for the formation of multiple sets by the rotation of faults and blocks. The model predicts four features to the study area.

a) Crustal deformation is accommodated by right lateral strike slip faults

b) The observed paleomagnetic rotation requires at least two, and possibly three, sets of faults.

c) The angle $\varnothing_c$ between the sets of faults should be in the range of 25° to 45°.

d) The angle between the oldest and youngest sets of faults has the same sense of, and is equal to the measured paleomagnetically derived total rotation.

The structural data show that fault slip is predominantly right lateral strike slip, consisting of three fault sets, with an angle of 39° between sets 1 and 2 and 46° between sets 2 and 3. The total structural rotation which is the sum of these two angles, is 85°. This value compares favorably with the 69° ± 13° of counterclockwise paleomagnetically derived rotation.

We conclude that the seemingly complex distributed strike slip fault pattern in the Mt. Hermon area is the result of large block rotations, which gave rise to three consecutive multiple fault sets. In this process older faults are systematically offset by younger sets, having identical slip sense.

The results are probably indicative of a general process of formation of multiple intersecting fault sets in the earth's crust. The multiple set model provides a simple and rational method for analyzing some very intricate fault patterns which, at first glance, appear very complicated and are often assumed to require an incredibly complex stress history to explain their formation.

REFERENCES

Angelier, J., 1985, Tectonic analysis of fault slip data sets. J. Geophys. Res., 89, p. 5835-5848.

Ben Menhem, A., Nur, A., and Vered, M., 1976, Tectonics, seismicity and structure of the Afro-Eurasian junction - the breading of an incoherent plate. Phy. of the Earth and Planet. Inter., 12, p. 1-50.

Byerlee, J. D., 1978, Friction of rock. Pure and Appl. Geophys., 116. p. 615-626.

Eyal, Y., and Reches, Z., 1983, Tectonic analysis of the Dead Sea Rift region since the Late Cretaceous based on mesostructures. Tectonics, 2, p. 167-185.

Fisher, R. A., 1953, Dispersion on a sphere. Proc. R. Soc., London, Ser. A, 217, p. 295-305.

Freund, R., Garafunkel, Z., Zak, I., Goldberg, M., Weissbrod, T., and Derin, B., 1970, The shear along the Dead Sea Rift. Philos. Trans. R. Soc., London, Ser. A., A267, p. 107-130.

Freund, R., 1974, Kinematics of transform and transcurrent fault. Tectonophysics, 21, p. 93-134.

Gans, P. D., and Miller, E. I., 1983, Style of mid-Tertiary extension in east central Nevada, in Guidebook part 1, Geological Society of American Rock

Mountain and Cordilleran Section Meeting, Utah. Geology and Mining Survey Special studies, V. 59, p. 107-160.

Garfunkel, Z., 1974, Model for the late Cenozoic tectonic history of the Mojave Desert, California and its relation to adjacent areas. Geological Society of America Bulletin, V.85, p. 1931-1944.

Garfunkel, Z., 1981, Internal structure of the Dead Sea leaky transform (rift) in relation to plate kinematics. Tectonophysics, 80 (1-4), p. 84-108.

Gregor, C. B., Mertzman, S., Narin, A. E. M., and Negendank, J., 1974, Paleomagnetism of some Mesozoic and Cenozoic volcanic rocks from the Lebanon. Tectonophysics, 21, p. 375-395.

Hancock, P. L., and Atyla, M. S., 1979, Tectonic significance of the mesofractures systems associated with the Lebanese segment of the Dead Sea Transform Fault. J. Struct., Geol., 1, p. 143-153.

Jaeger, J. D., and Cook, N. G. W., 1976, Fundamentals of rock mechanics. John Wiley & Sons Inc., New York, p. 585.

Joffe, S., and Garfunkel, Z., 1987, Plate kinematics of the circum Red Sea; a re-evaluation. Tectonophysics, 141, p. 5-22.

Menton, W. I., 1987, Tectonic interpretation of the morphology of Honduras. Tectonics, V. 6, No.5, p. 633-651.

Nicholson, C., Seeber, L., Williams, P. L., and Sykes, L. R., 1986, Seismicity and fault kinematics through the eastern Transverse Range, California block rotation, strike slip faulting and low angle thrusts. Journal of Geophysical Research, V. 91, p. 4891-4898.

Nur, A., Ron, H., and Scotti, O., 1986, Fault mechanics and the kinematics of block rotation, Geology, 14, p. 746-749.

Proffett, J. M., Jr., 1977, Cenozoic geology of the Yerington district, Nevada and implications for the nature and origin of Basin and Range faulting. Geological Soc., of American Bull., 88, p. 247-266.

Ron, H., 1987, deformation along the Yammuneh, the restraining bend of the Dead Sea. Transform; paleomagnetic and kinematic implications. Tectonics, 6, p. 653-666.

Ron, H., Aydin, A., and Nur, A., 1986, Strike-slip faulting and block rotation in the Lake Fault system. Geology, V.14, p. 1020-1023.

Ron, H., Freund, R., Garfunkel, Z., and Nur, A., 1984, Block rotation by strike slip faulting; structural and paleomagnetic evidence. Journal of Geophysical Research, 89, p. 6265-6270.

Stamatakos, J. A., Kodama, K. P., and Pavils, T. L., 1988, Paleomagnetism of Eocene plutonic rocks, Matanusak Valley, Alaska. Geology, V.16, p. 618-622.

Terres, R. R., and Luyendyk, B. P., 1985, Neogene tectonic rotation of the San Gabriel region, California, suggested by paleomagnetic vector. Journal of Geophysical Research, V. 90, p. 12467-12484.

FIGURE CAPTIONS

Figure 1. Block rotation model of multiple strike slip sets, showing a new fault set required to accommodate block rotation greater than 45°. The angle $\varnothing_o$ is the initial angle of the first set and $\varnothing_c$ is the angle between the first and second new sets (after Nur et. al., 1986).

Figure 2. General plate tectonic setting of the study area (a) and conceptual geometrical reconstruction of faulting and rotation of the investigated area (b) before fault slip and (c) after fault slip.

Figure 3. Equal area projection of poles and rose diagrams of all faults in the Mt. Herman area.

Figure 4. Equal area projection and rose diagram of all right lateral strike slip faults in Mt. Hermon area.

Figure 5. Equal area projection of all right lateral strike slip faults in the Mt. Hermon area after separation into three distinct populations.

Figure 6. Equal area projection and rose diagram of all left lateral strike slip faults in the Mt. Hermon area. All faults and planes were projected to the west.

Figure 7. Equal area projection of all left lateral strike slip faults in the Mt. Hermon area after separation into three distinct populations.

Figure 8. Equal area projection and rose diagram of all right lateral strike slip faults in Neve Ativ (NA) outcrops.

Figure 9. Equal area projection of all right lateral strike slip faults in Neve Ativ (NA) area after separation into three distinct populations. Separation was based on crosscut field relation of the faults.

Figure 10. Mean plane for the three right lateral fault population of (a) NA outcrop and (b) Mt. Hermon area. Mean poles were plotted with the circle of A95 confidence. $\varnothing_c$ is the angle between the fault sets.

SUMMARY OF STRUCTURAL DATA

AREA	FAULT SET	FAULT STRIKE	FAULT DIP	A95	ANGLUAR SD	N	$\varnothing_c$
REGIONAL							
Hermon	1st.	253	89	6	20	49	39
Hermon	2nd.	293	86	6	20	49	46
Hermon	3rd.	339	83	7	24	51	
LOCAL							
NA1	1st.	256	82	5	22	26	27
NA2	2nd.	283	88	10	21	25	47
NA3	3rd.	330	80	7	16	15	

Table 1. Statistical parameters of the right lateral strike slip faults on the study area. N is the number of faults in each population. A95 is the 95% confidence about the mean and $\varnothing_c$ is the angle between the fault sets. Hermon-regional includes all right lateral faults in the study area. Neve Ativ-local includes only faults of this local outcrop.

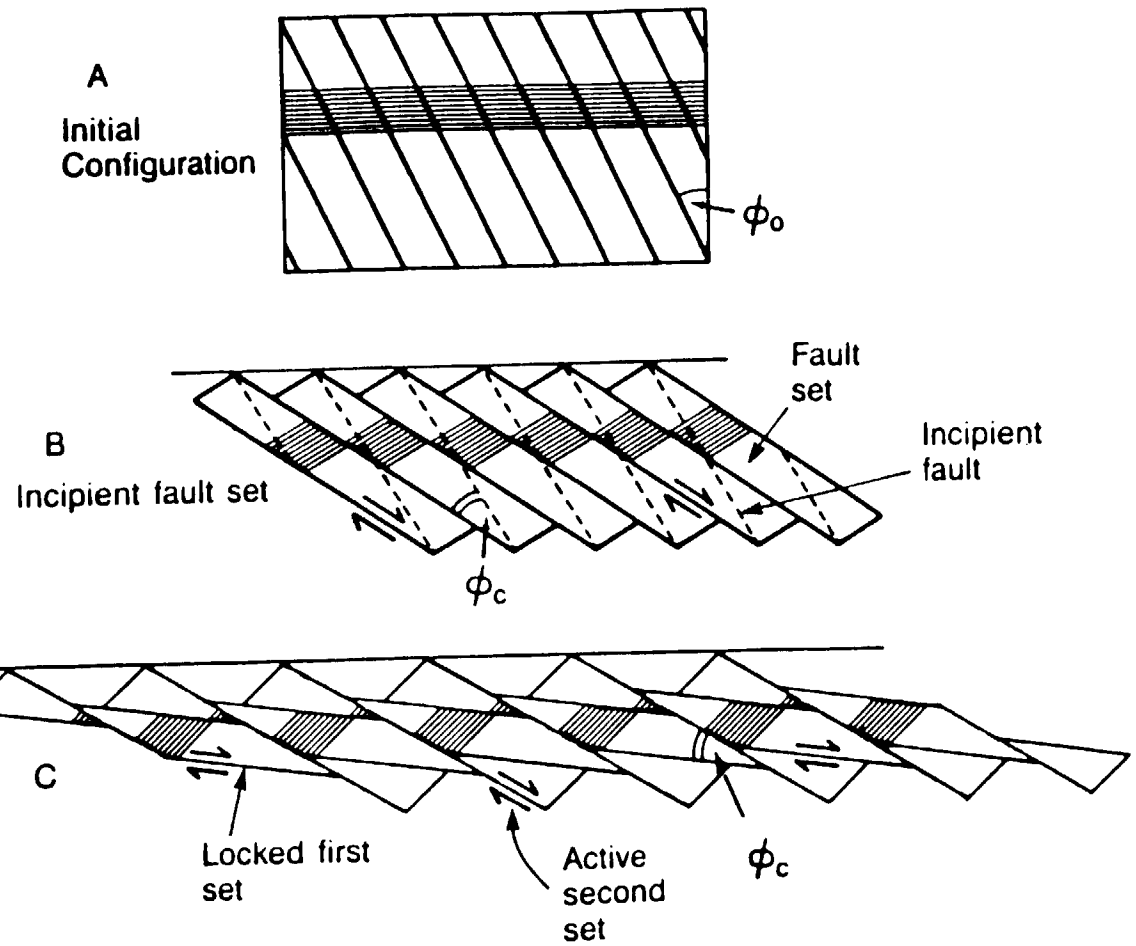
A
Initial
Configuration
ϕ_o
B
Incipient fault set
Fault
set
Incipient
fault
ϕ_c
C
Locked first
set
Active
second
set
ϕ_c

fig 1

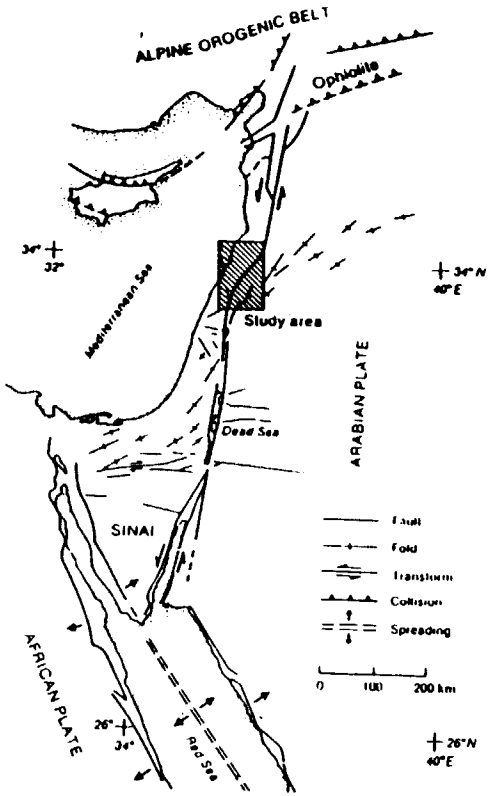

a

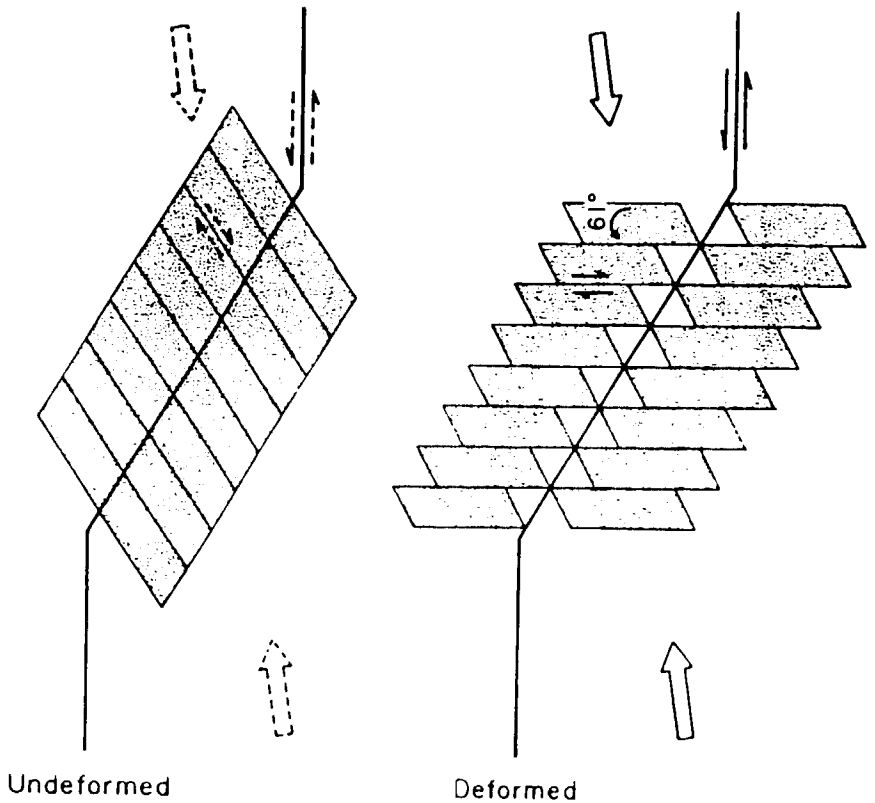

b

fig 2

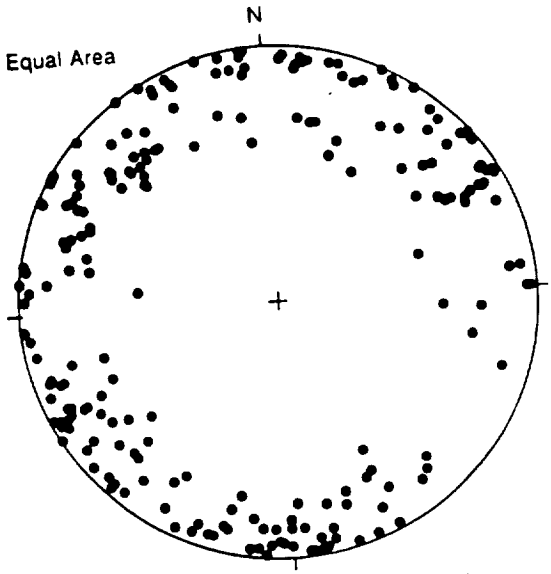

HERMON - POLE DISTRIBUTION
OF ALL FAULTS

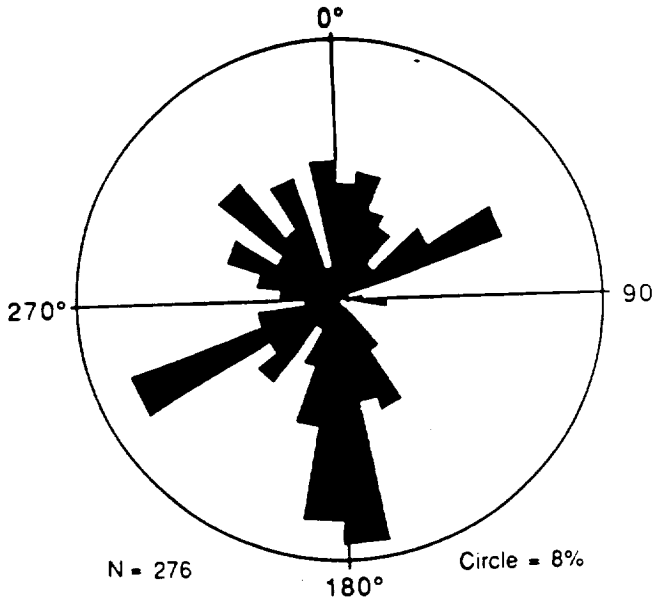

ROSE DIAGRAM OF POLE TREND:
HERMON - ALL FAULTS

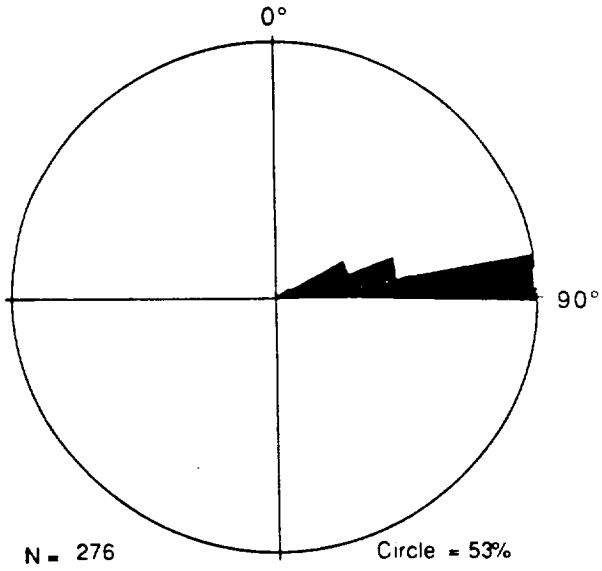

ROSE DIAGRAM OF DIP ANGLE FOR
HERMON - ALL FAULT PLANES

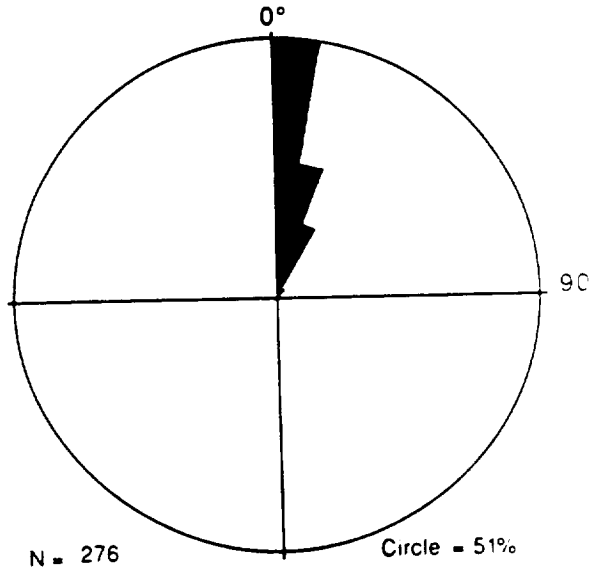

ROSE DIAGRAM OF DIP ANGLE FOR
HERMON - RAKE OF ALL FAULTS

fig 3

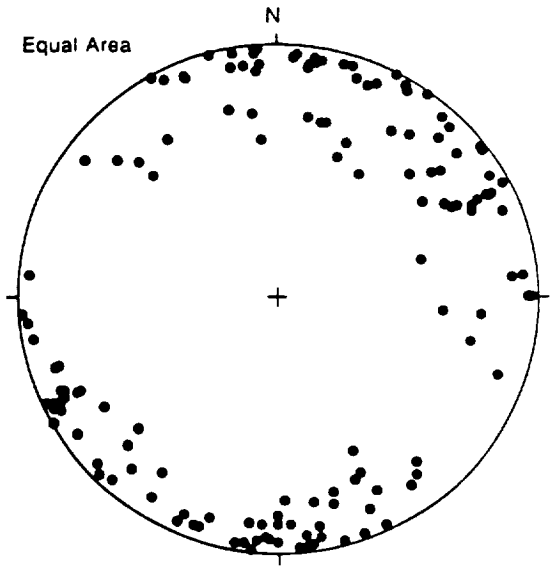

DISTRIBUTION OF POLE FOR
HERMON - ALL RIGHT LATERAL SSF

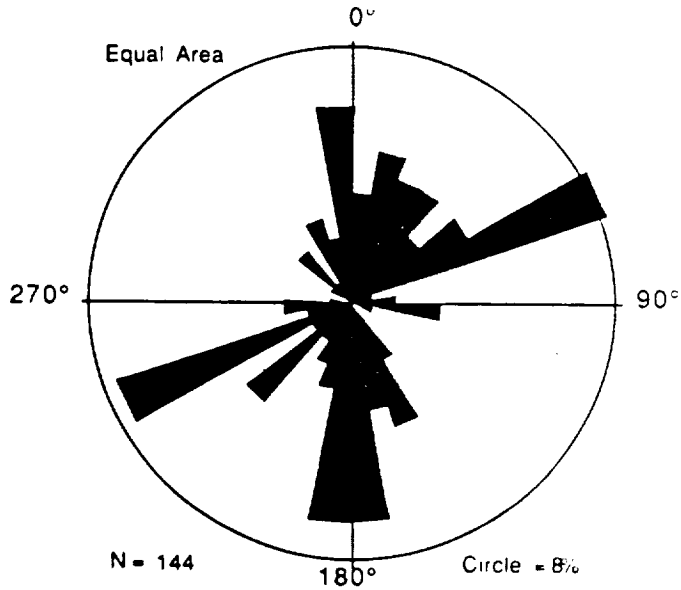

ROSE DIAGRAM OF POLE TREND FOR
HERMON - ALL RIGHT LATERAL SSF

fig 4

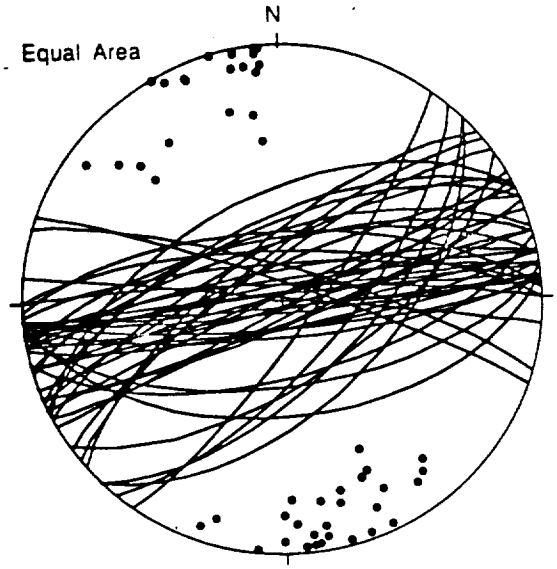

DISTRIBUTION OF PLANES AND POLES FOR
HERMON - 1ST SET OF RIGHT LATERAL SSF

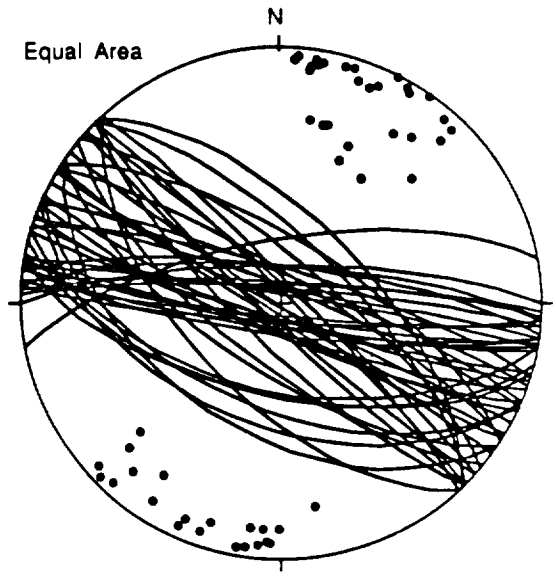

DISTRIBUTION OF PLANES AND POLES FOR
HERMON - 2ND SET OF RIGHT LATERAL SSF

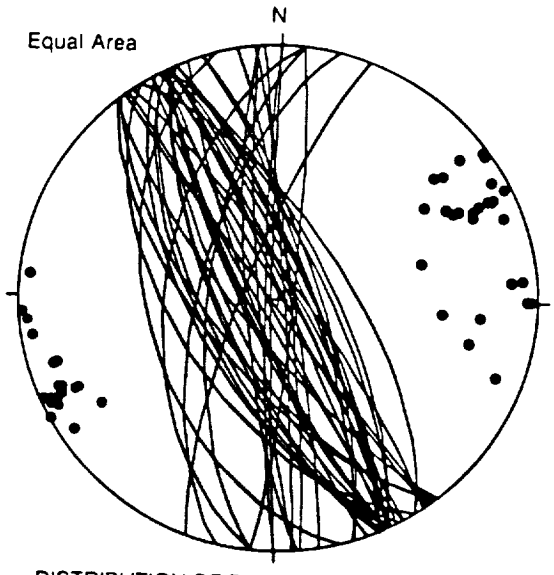

DISTRIBUTION OF PLANES AND POLES FOR:
HERMON - 3RD SET OF RIGHT LATERAL SSF

fig 5

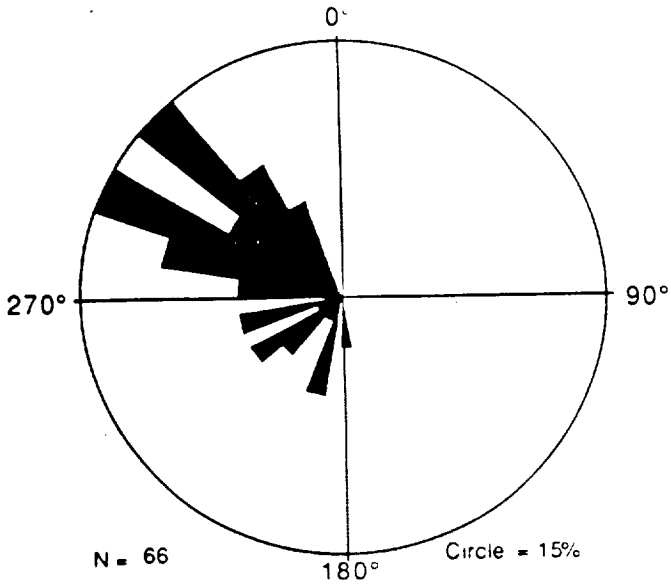

ROSE DIAGRAM OF POLE TREND FOR
HERMON - ALL LEFT LATERAL SSF

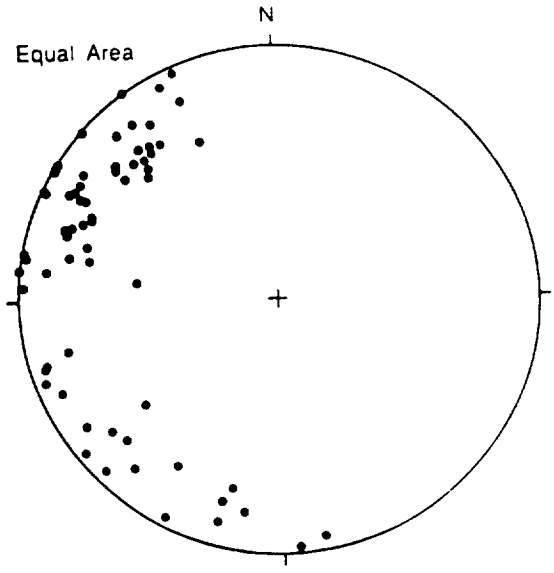

DISTRIBUTION OF POLE FOR
HERMON - ALL LEFT LATERAL SSF

fig 6

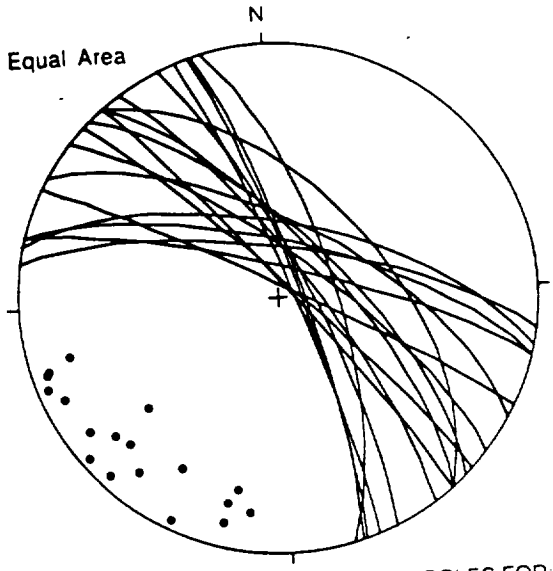

DISTRIBUTION OF PLANES AND POLES FOR:
HERMON - 1ST SET OF LEFT LATERAL SSF

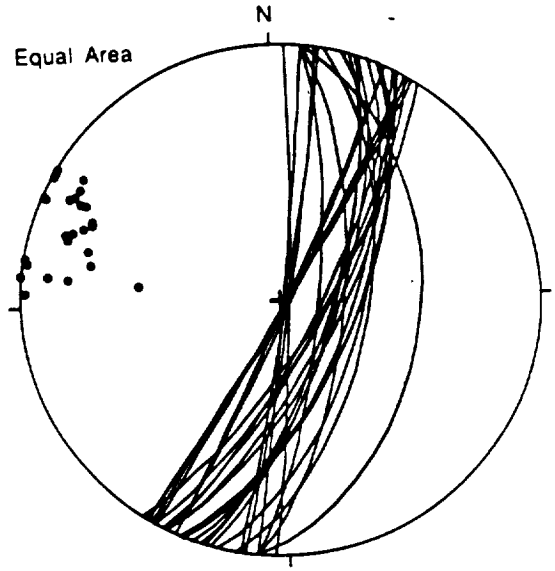

DISTRIBUTION OF PLANES AND POLES FOR:
HERMON - 2ND SET OF LEFT LATERAL SSF

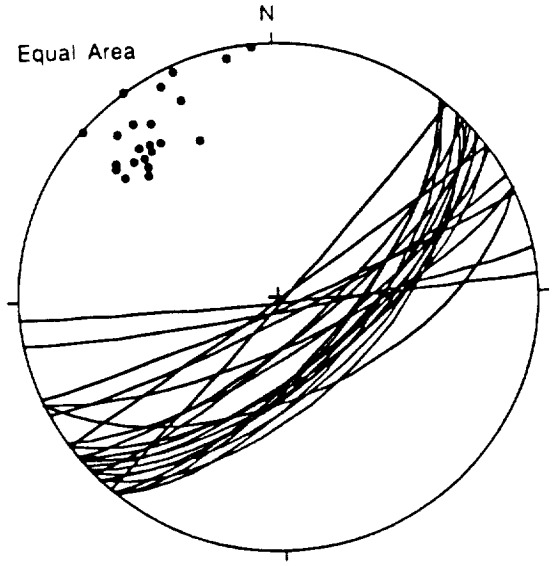

DISTRIBUTIN OF PLANES AND POLES FOR:
HERMON - 3RD SET OF LEFT LATERAL SSF

fig 7

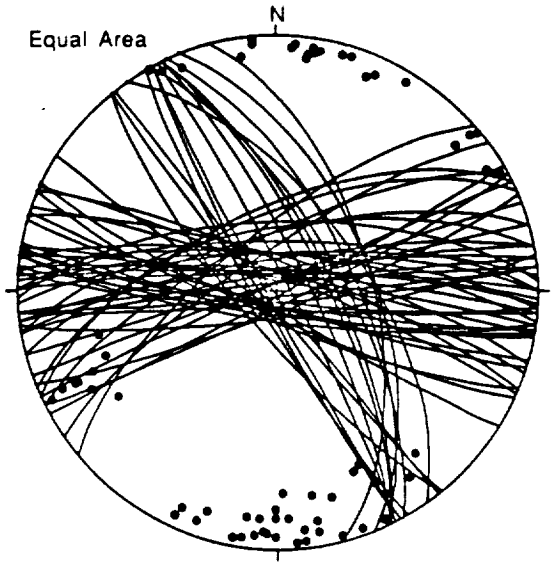

DISTRIBUTION OF PLANES AND POLES FOR:
NEVE ATIV - ALL RIGHT LATERAL SSF

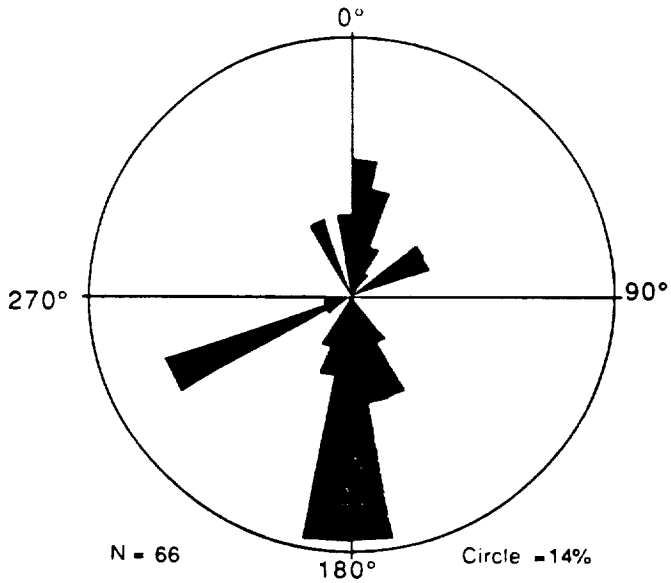

ROSE DIAGRAM OF POLE TREND DISTRIBUTION:
NEVE ATIV - ALL RIGHT LATERAL SSF

fig 8

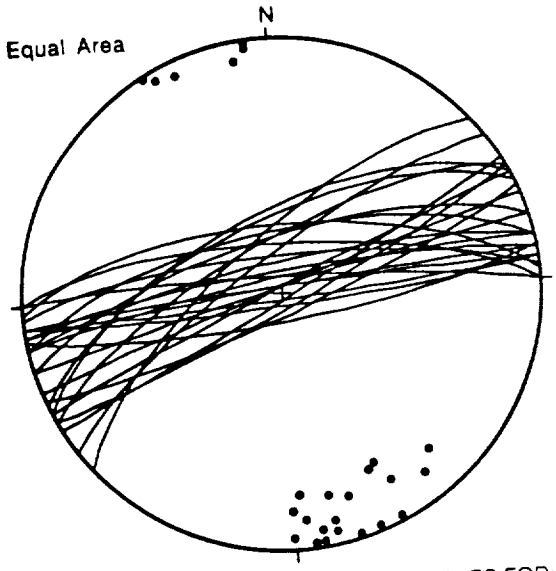

DISTRIBUTION OF PLANES AND POLES FOR:
NEVE ATIVE - 1ST SET OF RIGHT LATERAL SSF

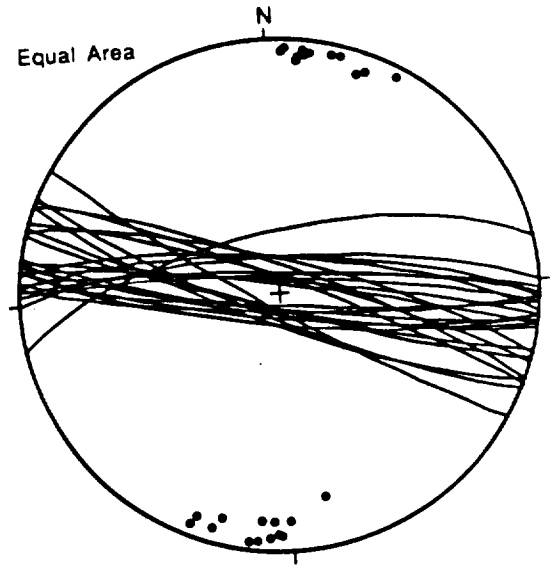

DISTRIBUTION OF PLANES AND POLES FOR:
NEVE ATIV - 2ND SET OF RIGHT LATERAL SSF

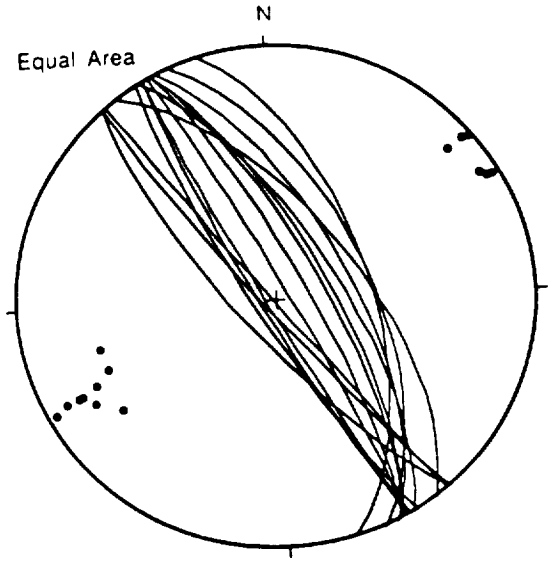

DISTRIBUTION OF PLANES AND POLES FOR:
NEVE ATIV - 3RD SET OF RIGHT LATERAL SSF

fig 9